

The Suitability of Monopolar and Bipolar Ion Exchange Membranes as Separators for Biological Fuel Cells

FALK HARNISCH, UWE SCHRÖDER,* AND FRITZ SCHOLZ

Institute of Biochemistry, University of Greifswald, Felix-Hausdorff-Strasse 4, 17487 Greifswald, Germany

Received September 6, 2007. Revised manuscript received December 5, 2007. Accepted December 7, 2007.

A proton exchange (Nafion-117), a cation exchange (Ultrax CMI7000), an anion exchange (Fumasep FAD), and a bipolar (FumasepFBM) membrane have been studied to evaluate the principle suitability of ion exchange membranes as separators between the anode and the cathode compartment of biological fuel cells. The applicability of these membranes is severely affected by the neutral pH, and the usually low ionic strength of the electrolyte solutions. Thus, the ohmic resistance of the monopolar membranes was found to greatly increase at neutral pH and at decreasing electrolyte concentrations. None of the studied membranes can prevent the acidification of the anode and the alkalization of the cathode compartment, which occurs in the course of the fuel cell operation. Bipolar membranes are shown to be least suitable for biofuel cell application since they show the highest polarization without being able to prevent pH splitting between the anode and cathode compartments.

Introduction

Since the introduction of polymer electrolyte (or proton exchange) membrane fuel cells (PEMFC), proton exchange membranes (PEM) have become a vital part of low temperature fuel cells, serving as separators between the anode and the cathode compartment while assuring the charge balancing proton transfer from the anode to the cathode. Major reasons for the success of the PEM's are their high proton conductivity, high chemical stability, and a comparably low permeability for oxygen and most fuels (1, 2).

Apart from exceptions like benthic (microbial) fuel cells (3, 4), in which the interface between seawater and sediment serves as natural boundary between anode and cathode, and a number of enzymatic fuel cells, which due to the immobilization of the highly specific biocatalysts at the respective electrodes allow a membrane-free design (5), the great majority of biological fuel cells—like chemical fuel cells—require a diaphragm between the anode and cathode compartments, e.g., ref 6.

Derived from chemical fuel cells, the use of polymer electrolyte membranes like Nafion was adopted also to biological fuel cells, assuming that the charge balancing ion transfer between anode and cathode compartment is realized in the form of proton transfer, according Figure 1. Yet, recently, it has become increasingly obvious that the simplified conception of a purely proton-based ion transfer does

not, or only to a minor extent, apply to biofuel cells (7, 8). As a consequence of the biological nature of the catalysts, microbial and enzymatic fuel cells generally operate at pH values near 7 (corresponding to a proton concentration of 10^{-7} mol L⁻¹), and the ionic conductivity is attained mainly using alkali metal salts and buffers in a concentration range between 10^{-3} and 10^{-1} mol L⁻¹. The concentration ratio of alkali ions to protons can thus be as high as 10^6 .

In a number of recent papers it has been described that this great excess of metal cations leads to a significant contribution of these ions to the charge balancing ion transfer across the separating membrane—from the anodic to the cathodic fuel cell compartment (7–9). It has to be noticed that proton exchange membranes of the Nafion type possess a preferential conductivity for protons, but the conductivity ratio is as low as 3.4 for H⁺/Na⁺ and 6.2 for H⁺/K⁺ for Nafion-117 (10). The nonproton cation transfer leads to an accumulation of protons in the anodic compartment (decrease of pH) and an increase of pH in the cathodic compartment. The consequences are severe: first of all, an increasing deviation of the pH from physiological values leads to a decreasing biocatalyst activity and may even cause full deactivation. In a microbial fuel cell this may mean the decrease of biocatalysts activity and in enzymatic fuel cells the denaturation of the isolated redox enzymes. Second, the occurrence of a pH gradient leads to a considerable decrease of the thermodynamic cell potential. The reason for this is the involvement of protons in the anode and cathode reactions. Thus, most anode reactions are proton liberating processes (e.g., the oxidation of glucose to gluconic acid, the oxidation of hydrogen or oxidation of microbial mediators like pyocyanine) (11). Assuming a one proton, one electron oxidation, a pH decrease of one unit would lead to a shift of the anode potential of +59 mV (assuming nernstian behavior). The cathodic oxygen reduction on the other hand is proton consuming; here, the increase of the pH leads to a negative potential shift (–59 mV/pH unit). Especially in the case of MFC air cathodes, pH values of up to 13 have been reported, which can be attributed to the low volume of permeated electrolyte at the cathode side (12).

Different strategies have been proposed to circumvent the problem of the opposite pH change in the cell compartments. Thus, for microbial fuel cells, the use of pH-static control (7) or of membrane-free configurations (13, 14) have been suggested. The first approach requires controlled continuous addition of bases to the anode and acids to the cathode chamber—a technical and operational cost factor that may not be justifiable; the other approach suffers from comparably low Coulombic efficiencies due to oxygen crossover into the anode compartment. As an alternative strategy, the use of membrane materials such as cation exchange membranes (CEM), anion exchange membranes (AEM), bipolar membranes (BPM), and ultracentrifugation membranes (UCM) has been proposed and studied by different groups in microbial fuel cell experiments (12, 15, 16). These experiments, however, allowed the operational parameters to be varied only in a narrow range. They delivered information on the overall biofuel cell performance but did not provide information on the principle suitability of ion exchange membranes as biofuel cell separators and the conditions under which this suitability would apply.

This paper examines the principle suitability of monopolar and bipolar polymer electrolyte membranes for application in biological fuel cells. It discusses basic membrane properties like the polarization behavior and shows how the different ways of migrative and diffusive ion transport through the

* Corresponding author phone: +49-3834-864330; fax: +49-3834-864451; e-mail: uweschr@uni-greifswald.de.

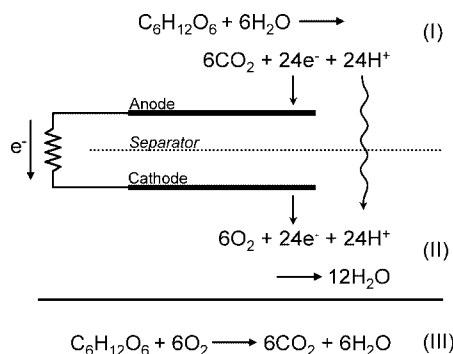


FIGURE 1. Simplified model of anodic and cathodic reactions and the charge balancing ion transfer in a biological fuel cell.

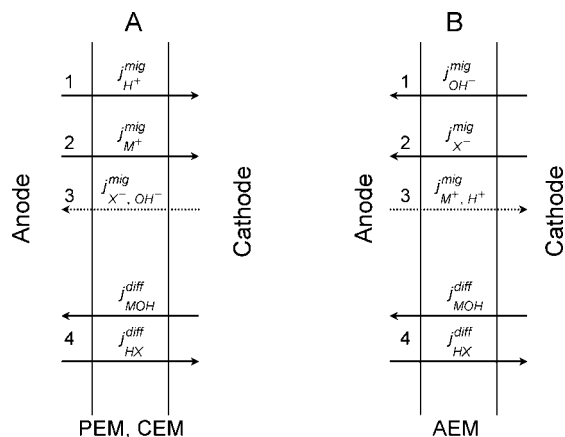


FIGURE 2. Schematic illustration of the major migrative (j^{mig}) and diffusive (j^{diff}) fluxes across cation (A) and anion (B) exchange membranes.

ion exchange membranes affect the operation and the performance of biological fuel cells.

To ensure a high degree of experimental variability, e.g., with respect to current densities, electrolyte composition, and pH, an experimental approach based on an (abiotic) electrolysis cell (two-chamber) was chosen, instead of a fuel cell setup. Four different membranes, which represent the major relevant membrane types, were studied: Nafion-117 (PEM), Ultrex CMI-7000 (CEM), Fumasep-FAD (AEM), and Fumasep-FBM (BPM).

Fundamentals

Ion and Mass Transfer Processes Across Monopolar Membranes. For a better understanding of the phenomena reported in this article, the following sections will provide an introduction into the major ion and mass transfer processes across monopolar (CEM, PEM, AEM) and bipolar ion exchange membranes.

Monopolar ion exchange membranes are charge selective, i.e., they selectively transport either cations (including protons) (CEM, PEM) or anions (AEM) from one side of the membrane to the other.

For this purpose the membranes operate according to the principle of Donnan exclusion (17). The membranes consist of polymer networks containing immobilized, charged groups (e.g., $-\text{SO}_3^-$, $-\text{NR}_4^+$) that allow the transfer of oppositely charged ions, whereas the transfer of ions of the same sign as the immobilized groups is largely blocked. The ion transfer proceeds via migration, i.e., the ions are transferred in the electric field that builds up as the result of the anodic and cathodic reactions (see Figure 2A and B). For a CEM (and PEM) this means a preferable migration of cations (and H_3O^+), and for an AEM the preferable migration of anions (see solid

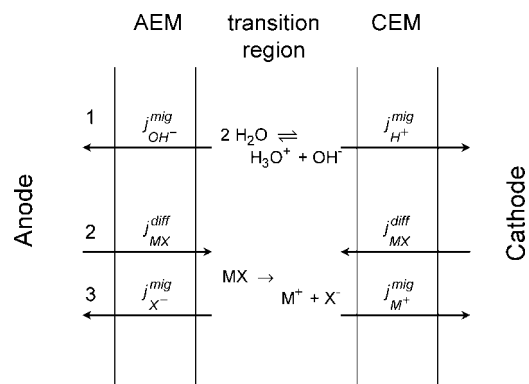


FIGURE 3. Schematic illustration of the structure of and the ion fluxes across a bipolar membrane.

arrows in Figure 2). To a minor extent (dashed arrows), a limited migration of anions (CEM) and cations (AEM) into the opposite direction takes place.

Additionally to the desired ion conductivity (permselectivity) all membranes are, to a certain extent, permeable to neutral species as gases (e.g., ref 18), organic compounds (e.g., ref 19), and electrolyte salts (e.g., ref 10). The cross-over of these species is diffusional and is caused by the concentration gradient between the anode and the cathode compartment.

Ion and Mass Transfer Processes Across Bipolar Membranes. Bipolar membranes consist of an anion exchange and a cation exchange layer mounted together as illustrated in Figure 3.

Ideally, the ionic conductivity of bipolar membranes are not the result of an ion flux across the membrane but of a water splitting reaction at the interface of (or in the transition region between) the anion and cation exchange membrane. The water splitting leads to the formation of protons and hydroxide ions, which then migrate through the CEM and the AEM layer, respectively (see Figure 3). To split water in protons and hydroxide anions using a bipolar membrane an energy of 22 W h is required (20). This energy corresponds to a membrane polarization of ~ 820 mV ($\Delta E = -\Delta G/F$) (21).

Due to the nonideal properties of the anion and cation exchange layers and the resulting permeability for electrolyte salts, the transition area (or interface) between the AEM and the CEM under equilibrium conditions always contains a certain concentration of electrolyte salts (illustrated as MX in Figure 3).

By applying an electric field, the electrolyte anions migrate through the AEM toward the anode, and the cations through the CEM toward the cathode. This ion flux is often referred to as leakage current, $j_{leakage}$. (22). It is not based on water dissociation. When all electrolyte ions are removed from the transition area, i.e., when the rate of ion migration out of the transition area exceeds that of the electrolyte diffusion into the transition area the membrane polarization increases and the water splitting reaction commences. The total ion flux is then composed of the contributions of the leakage current and the water splitting (23) (eq 1).

$$j_{ion, total} = j_{leakage} + j_{water\ splitting} \quad (1)$$

Experimental Section

Membranes. The following membranes were used throughout the experiments: Nafion-117 (DuPont), Ultrex CMI-7000 (Membranes International Inc., U.S.), Fumasep-FAD, and Fumasep-FBM (both Fuma-Tech GmbH, Germany).

The Nafion-117 membrane was treated in sulfuric acid and hydrogen peroxide before use (25). The other membranes were used as purchased. All membranes were stored in a 2

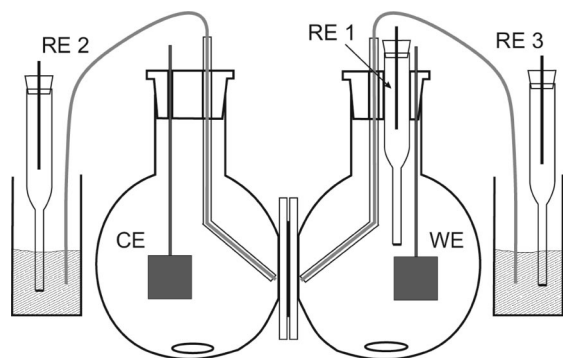


FIGURE 4. Schematic drawing of the two-chamber electrochemical cell for the study of membrane polarization and of the pH splitting.

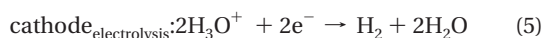
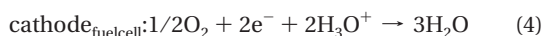
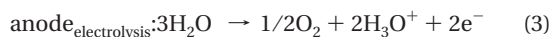
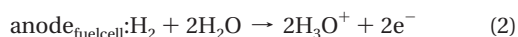
M NaCl solution in the dark to prevent biofouling and were rinsed thoroughly with deionized water before use.

Chemicals and Materials. All electrolyte solutions were prepared using deionized water. All chemicals (KH_2PO_4 , K_2HPO_4 , H_3PO_4 , KNO_3 , and HNO_3) were of analytical grade and were used as purchased (Aldrich, Fluka, and Merck).

Cell Design and Experimental Setup. All electrochemical experiments were carried out using a self-made two-chamber electrochemical cell (26) (Figure 4). It was composed of two 250 mL volume round-bottomed flasks pressed together at laterally inserted windows with an inner diameter of 2.3 cm. The membranes were clamped between the windows (sealed by rubber gaskets), leaving a geometric surface area of the membrane of 4.16 cm^2 . Both compartments contained a platinum mesh electrode (100 cm^2 approximate geometric surface area per electrode), serving as anode and cathode (working electrode and counter electrode, respectively). Additionally, the anode compartment was equipped with a reference electrode (RE 1, Ag/AgCl, sat. KCl, Sensortechnik Meinsberg, Germany, 0.195 V vs SHE) to allow three electrode based galvanostatic or potentiostatic control.

For the recording of the membrane polarization, two Luggin capillaries, connected via sat. KCl solutions to two external Ag/AgCl sat. KCl reference electrodes (Figure 4: RE 2, 3), were placed in identical distance of 1 mm to the membrane surface. The potential difference between both electrodes was measured with a battery driven, high-ohmic voltmeter (pH meter, Greisinger Electronic, Germany).

For a higher degree of experimental freedom, membrane polarization and pH splitting were not studied under fuel cell conditions but under the conditions of electrolysis. This approach is valid since, as illustrated in eqs 2–5, anodic proton liberation and cathodic proton consumption proceed analogously:



For simplification, eq 2 illustrates the fuel cell anode reaction by means of the oxidation of hydrogen; however, the anodic proton liberation can well be generalized for the oxidation of organic matter in biological fuel cells according to Figure 1(I).

Under the condition of electrolysis, electrolyte species could potentially be involved in the electrochemical oxidation or reduction reactions, which would possibly lead to a deviation in the proton production/consumption balance in the anode and cathode compartment, respectively. To exclude a contribution of reduction processes of nitrate (used

as a standard electrolyte anion in this study) we have determined the concentration of nitrate in the course of the electrochemical experiments via ion chromatography. In these experiments, however, we could neither see any decrease of nitrate concentration nor the formation nitrite.

Electrochemical Instrumentation. Galvanodynamic linear sweep voltammetry and chronoamperometry were carried out in conventional three electrode arrangements using Autolab systems (PGSTAT 30, EcoChemie, Netherlands) interfaced to a personal computer. The measurement of electrolyte pH and membrane polarization was conducted using battery driven, high-ohmic voltmeter (pH meter, Greisinger electronic, Germany).

For the continuous recording of the pH changes in the anode and cathode chambers, the pH data were logged using a data acquisition system (Integra 2700 series (Keithley Instruments, Inc., Cleveland) equipped with 7700 multiplexer,) interfaced to a personal computer.

The solution resistance was determined using a standard digital conductometer (Qcond 2200).

Experimental Conditions. All current density data, j_M , in this publication refer to the geometrical surface areas of the ion exchange membranes. The majority of measurements was performed in a current density range of $0 < j_M < 5 \text{ mA cm}^{-2}$, which is the range that is relevant for biological fuel cells, e.g., refs 27 and 28. To ensure steady state conditions, the galvanodynamic measurements were carried out at very low scan rates (0.05 mA s^{-1}).

For the determination of the membrane polarization, E_M , the potential difference measured between the tips of the Luggin capillaries, E_{exp} , was corrected by the value of the solution resistance, according to eq 6.

$$E_M = E_{\text{exp}} - j_M \times \rho_{\text{electrolyte}} \times L \quad (6)$$

($\rho_{\text{electrolyte}}$ represents the specific resistivity of the electrolyte solution, determined via conductivity measurements; L is the mean distance between the tips of both Luggin capillaries and the membrane).

The H^+ transport number, β_{H^+} , reflects the number of protons transferred from the anode to the cathode compartment in relation to the overall electric charge (eq 7). For the measurement of the H^+ transport number under different conditions, a fixed charge of 10 C was transferred and the pH change in anode and cathode compartment was monitored.

$$\beta_{\text{H}^+} = \frac{n_{\text{H}^+}}{n_e} = 1 - \frac{VF\Delta c_{\text{H}^+}^{\text{cathode}}}{Q} \quad (7)$$

(V represents the volume of the electrolyte solution, F is the Faraday constant, and Q is the electric charge).

All experimental data in this publication are based on at least three replications of the respective experiments. The standard deviations were as follows: for polarization values below 20 mV: $\pm 3 \text{ mV}$, for polarization values between 20 mV, and 50 mV $\pm 5 \text{ mV}$; for polarization values above 50 mV the standard deviation was below $\pm 10 \text{ mV}$. From these values the standard deviation of the resistance values were calculated being below $\pm 5\%$.

Results and Discussion

Membrane Polarization. Figure 5 depicts the principle shape of the polarization curves of monopolar and bipolar ion exchange membranes at low current densities and at neutral pH. The figure clearly illustrates the fundamental difference between in the polarization behavior. As expected, monopolar ion exchange membranes yield a linear polarization plot, the slope of which gives the ohmic resistance, R_{membr} , of the respective membrane. Based on the underlying water splitting reaction, the polarization curve of the bipolar membrane is

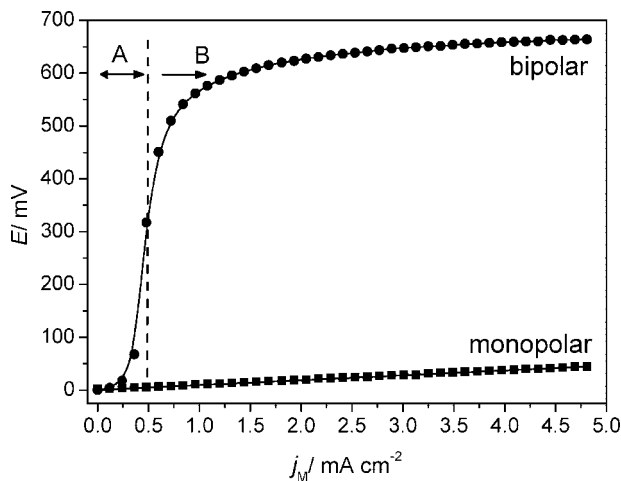


FIGURE 5. Polarization behavior of monopolar (Nafion-117, PEM) and bipolar (Fumasep-FBM, BPM) ion exchange membranes as a function of the current density, j_M , pH neutral electrolyte solution (100 mM KNO_3).

TABLE 1. Basic Membrane Properties^a

	type	thickness (μm)	ohmic resistance ($\Omega \text{ cm}^2$)
Nafion-117	PEM	183	15 ^b
Ultrex CMI-7000	CEM	457	<30 ^{a, c}
Fumasep-FAD	AEM	80-100	<1 ^{a, c}
Fumasep-FBM	BPM	180	<3 ^{a, d}

^a Manufacturer information. ^b AC measurement, 0.5 M NaCl, 24. ^c In 0.5 M NaCl. ^d 0.5 M H_2SO_4 , starting at 50 mA cm^{-2} .

TABLE 2. Ohmic Resistances and Specific Resistances of the Tested Membranes in in 0.05 M, pH 7, $\text{K}_2\text{HPO}_4/\text{KH}_2\text{PO}_4$ Electrolyte Solutions^a

type	brand	$R_{\text{membrane}}/\Omega \text{ cm}^2$	$\rho_{\text{membrane}}/\Omega \text{ cm}^*$
AEM	Fumasep-FAD	12.4	1378
CEM	Ultrex CMI-7000	45.1	987
PEM	Nafion-117	9.2	503

^a Calculated as $P_{\text{membrane}} = R_{\text{membrane}}/L$, with L being the respective thickness of each membrane (table 1).

sigmoidally shaped and shows a considerably higher polarization than monopolar membranes.

Table 2 provides an exemplary selection of measured resistance values for the tested monopolar membranes for pH 7 phosphate buffer solutions. The ohmic resistance of the membranes varies between 9.2 $\Omega \text{ cm}^2$ (Nafion, PEM) and 45 $\Omega \text{ cm}^2$ (Ultrex, CEM). With the exception of the anion exchange membrane, these results follow the conductivity graduation expected from literature (24) and from the manufacturers' information (Table 1).

The large resistance of the Ultrex CEM may be attributed to its thickness: with 457 μm it is much thicker than the other monopolar membranes. The specific resistances, ρ_{membrane} , provide a measure for the conductivity independent of the membrane thicknesses. These data show a performance of the cation exchange membrane material in the range of the other materials.

The ion conductivity of the membranes and thus their resistance strongly depend on the nature of the electrolyte ions. This can be demonstrated for the example of the anion exchange membrane: In potassium nitrate solution (0.1 M) the resistance was 1 $\Omega \text{ cm}^2$ (111 $\Omega \text{ cm}$), complying with the

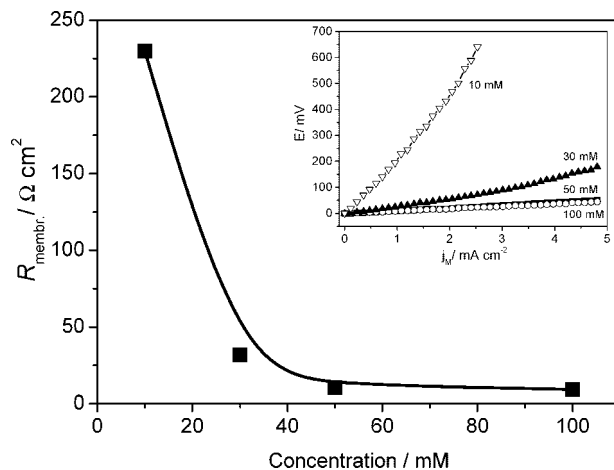


FIGURE 6. Main figure: Ohmic membrane resistance of Nafion-117 as function of the phosphate buffer concentration ($\text{KH}_2\text{PO}_4/\text{K}_2\text{HPO}_4$, pH 7). Inset figure: Polarization behavior of a Nafion membrane at different phosphate buffer concentrations.

manufacturer information (Table 1). In phosphate buffer solution, however, the ohmic resistance increased to 12.4 $\Omega \text{ cm}^2$ (1378 $\Omega \text{ cm}$).

The membrane resistance (and thus polarization) depends not only on the nature of the electrolyte ions but also on the pH and the concentration of the electrolyte solution.

As Figure 6 and Table 3 depict for the example of the Nafion-117 membrane the resistance of Nafion increases dramatically from about 0.33 $\Omega \text{ cm}^2$ at pH 1 (0.1 M HNO_3) to 230 $\Omega \text{ cm}^2$ in 10 mM, pH 7 phosphate buffer solution. This represents a resistance increase by a factor of 700. In contrast, the resistance of the electrolyte solutions increases only by a factor of 70 (table 3).

The polarization plot of the bipolar membrane can be divided into two sections, as illustrated in Figures 5 and 7. At low current density, the current flow is based on the leakage current, i.e. it is based on the diffusion of the electrolyte salt into the BPM and the subsequent migration of the respective ions through the AEM and CEM layer. Only when the electrolyte salt diffusion into the membrane cannot sustain the ion migration out of the membrane, the potential raises until water splitting occurs. The level of the leakage current (i.e., the extent of region A, Figure 6) is determined by the concentration of the electrolyte solutions and the permeability of the membrane for the respective electrolyte. As Figure 7 illustrates for the variation of the electrolyte pH, the leakage current can become as high as 2 mA cm^{-2} . It can be expected that in a previously reported use of a BPM in a microbial fuel cell (16) the leakage current represented the major charge balancing ion transfer process. The occurrence of the leakage current may prevent the considerably voltage losses that would occur as a result of the water splitting, yet, it has severe consequences on the pH balance between anode and cathode compartment (see next section).

pH Splitting Across the Separating Membrane. Figure 8 depicts a typical course of the pH values in the anode and the cathode chamber of an electrolytic cell as the result of a constant current flow. The figure clearly shows the development of the pH values of the anode and the cathode compartments in opposite directions, whereas the pH in the anode compartment decreases, the cathode pH increases significantly. At the end of the experiment, the pH difference between anode and cathode compartment, $\Delta\text{pH}_{\text{total}}$, was 9.8. Illustrated for the Nafion-117 proton exchange membrane as the separator between the half-cells, the depicted behavior is also found for all other tested membrane materials, including the bipolar membrane.

TABLE 3. Ohmic Resistance and Specific Resistance of Nafion 117 in Different Electrolyte Solutions and the Specific Electrolyte Resistance Values

	$R_{\text{membrane}}/\Omega \text{ cm}^2$	$\rho_{\text{membrane}}/\Omega \text{ cm}^*$	$\rho_{\text{membrane}}/\Omega \text{ cm}$
pH 1 (0.1 M HNO ₃)	0.33	18.0	10
pH 2.5 (0.1 M HNO ₃ /KNO ₃)	6.6	360.7	68.5
pH 7 (0.1 M KNO ₃)	17.6	961.7	95.2
pH 7 (0.1 M KH ₂ PO ₄ / K ₂ HPO ₄)	9.2	502.7	86.9
pH 7 (0.05 M KH ₂ PO ₄ / K ₂ HPO ₄)	10.5	573.8	142.5
pH 7 (0.03 M KH ₂ PO ₄ / K ₂ HPO ₄)	32.6	1781	260.4
pH 7 (0.01 M KH ₂ PO ₄ / K ₂ HPO ₄)	230	12568	701.8

* Calculated as $P_{\text{membrane}} = R_{\text{membrane}}/L$, with L being the thickness of a Nafion 117 membrane of 0.0183 cm.

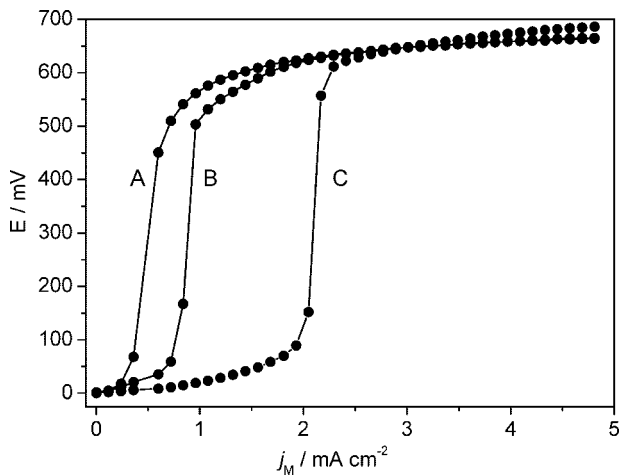


FIGURE 7. Polarization behavior of a bipolar membrane at different pH values. (A) pH 6 (0.1 M KNO₃); (B) pH 2.5 (0.1 M KNO₃/HNO₃); (C) pH 1(0.1 M HNO₃).

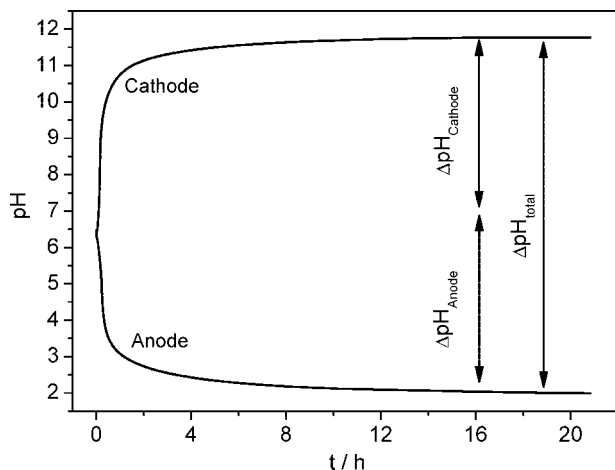


FIGURE 8. Course of the pH values in the anode and the cathode compartments during a galvanostatic experiment. The electrolyte was 50 mM KNO₃, the current density, j_M , was 1.2 mA cm⁻². Separator: Nafion-117.

This result has to be expected (22). It demonstrates that none of the membranes can prevent the pH splitting. Taking into account that the oxidation of one glucose molecule liberates 24 protons (see Figure 1), the full oxidation of a 50 mM glucose solution could accumulate a proton concentration of up to 1.2 mol L⁻¹ in the anode compartment (which will be equal to the hydroxide concentration in the cathode compartment). But what are the principle limits of the pH splitting?

The following scenarios will assume a pH 7 electrolyte solution of a certain concentration: When using a cation exchange membrane, the charge balancing ion transfer from

the anode to the cathode will be accomplished almost exclusively by the metal cations, as long as their concentration is considerably above that of the protons. In the course of the anodic oxidation processes protons accumulate in the anode compartment. The higher their concentration grows the more they are involved in the ion transfer until, once the proton concentration levels that of the metal ions, they become the predominantly transferred species. This assumption is confirmed in experiments in which, at high current densities (>10 mA cm²), the pH changes were monitored until stationary conditions were achieved. The end pH values in the anode compartment for 10⁻¹, 10⁻² and 10⁻³ M KNO₃ solutions were found to be 1.1, 2.0, and 3.2, respectively.

Logically, analogous processes will take place in the case of anion exchange membranes. Here, the predominant anionic species are transferred from the cathode to the anode, until the hydroxide concentration has increased to the level of the electrolyte salt.

Why are bipolar membranes not a solution to this problem? As explained in the fundamentals, bipolar membranes show a leakage current (Figures 5 and 7), caused by the diffusion of electrolyte salt into the membrane and the migration of the electrolyte ions through the respective membrane layer (Figure 3) (22). For the low current densities of biological fuel cells this leakage current is large compared to the total ion flux, and as in the case of CEM and AEM, it leads to the accumulation of protons at the anode and hydroxide at the cathode.

It can be suspected that in the study by ter Heijne et al. (16) the membrane was operated in the range of the leakage currents. Thus, the reported membrane polarization of ~200 mV of the bipolar membrane is similar to value obtained in our experiments for current densities below 0.3 mA cm⁻².

Are there possibilities to circumvent or at least to diminish the pH splitting when using ion exchange membranes? Figure 9 illustrates experiments in which a fixed charge of 10 C was transferred at different current densities. At the end of the experiment, the pH change was measured and was used to calculate the proton transfer number, $\beta_{\text{H}^+/\text{e}^-}$ (eq 7). This parameter provides information on the involvement of protons in the charge balancing ion transfer. A value of one means that the proton transport is the sole ion transport process, with the desired consequence of pH equilibrium between anode and cathode. The lower the value the larger are the pH changes in the fuel cell compartments. Figure 9 shows that for all membranes $\beta_{\text{H}^+/\text{e}^-}$ increases at decreasing current densities and decreases to a steady state value of about 0.1 at increasing current densities. The reason for the increase of the proton transfer number at low current density is the permeability of the respective membranes for diffusive mass transfer (see Figure 2). At low current density, increasing pH gradients between both electrode compartments lead to an increasing diffusion of the formed acids from the anode to the cathode and of the hydroxides from the cathode to the anode compartment. This neutralization leads to an increas-

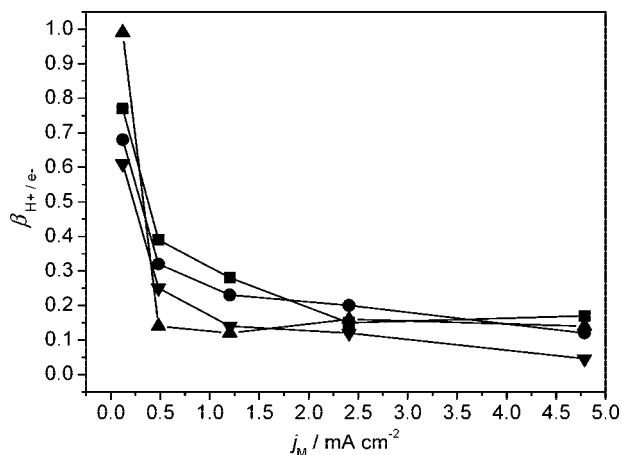


FIGURE 9. Dependence of the apparent proton transfer number on the current density for different membranes: (■) Nafion 117 (PEM); (●) Ultrex CMI-7000 (CEM); (▼) Fumasep-FAD (AEM); (▲) Fumasep-FBM (BPM). The electrolyte solution was 50 mM KNO_3 , the transferred charge was 10 C.

ing proton transfer number. Since the diffusion processes are slow compared to the migration of the charged ions (10) in the respective membranes, neutralization can be accomplished only at very low current densities.

The results of this study illustrate for the example of ion exchange membranes that the separation of the anode and the cathode compartment in biological fuel cells (enzymatic or microbial) entails the fundamental problem of the occurrence of a pH gradient between both fuel cell compartments. All studied ion exchange membranes show a similar behavior that is governed by the ratio of the solutions' pH to the electrolyte concentration. Due to the occurrence of large leakage currents, the use of bipolar membranes does not prevent the pH changes.

The effect of the pH changes can be reduced by operating on low current densities. Yet, this is not unrestrictedly advisable, since low current densities favor unwanted cross-over processes of either oxygen or substrates and may require large membrane surface areas.

The ohmic resistances of the monopolar membranes are all within a certain range. Yet, membrane resistances are not constants. Depending on the nature of the electrolyte salts the resistance values can vary considerably, even changing the order of resistance of the studied membranes. A major problem is the strongly increasing resistance at low ionic concentrations as applicable in natural environments. Here, the membrane resistance increases disproportionately high in comparison to the electrolyte resistance. The use of bipolar membranes cannot be recommended: Not only do they not prevent pH changes but their large polarization potential at higher current densities forbids their application.

A major conclusion of this study is that ion exchange membranes are only restrictedly suitable for application in biological fuel cells. It can, however, be assumed that the same applies to other separators, too. The ionic charge transport across the fuel cell separator will always be accomplished by the ionic species that are available at the highest concentration. In pH neutral buffer solutions, this is neither protons nor hydroxide ions. A higher porosity of material like nanoporous filters (14) may allow a faster neutralization, yet it may also result increasing crossover processes.

It emerges that innovative solutions are necessary to make the separator obsolete. Certainly, enzymatic fuel cells have an advantage, since the selectivity of their biocatalysts offers the possibility of membrane-free designs (5, 9). For microbial fuel cells, technological approaches have to be developed

that allow the increase of the Coulombic efficiency at membrane-free operation (29, 30).

Acknowledgments

F.H. gratefully acknowledges Ph.D. scholarships by the Deutschen Bundesstiftung Umwelt (DBU) and the Studienstiftung des deutschen Volkes. U.S. acknowledges support by the Deutsche Forschungsgemeinschaft (DFG). U.S. and F.S. additionally thank the Fond der Chemischen Industrie (FCI). The anion exchange membrane (FumasepFAD) and the bipolar membrane (FumasepFBM) were kindly provided by the Fuma-Tech GmbH, Germany.

Literature Cited

- (1) Kordesch, K.; Simander, G. *Fuel Cells and Their Applications*; Weinheim VCH: Weinheim, 1996.
- (2) Srinivasan, S. *Fuel Cells: From Fundamentals to Applications*; Springer Science & Business Media: New York, 2006.
- (3) Tender, L. M.; Reimers, C. E.; Stecher, H. A.; Holmes, D. E.; Bond, D. R.; Lovley, D. R. Harnessing microbially generated power on the seafloor. *Nat. Biotechnol.* **2002**, *20*, 821–25.
- (4) Reimers, C. E.; Tender, L. M.; Fertig, S.; Wang, W. Harvesting energy from the marine sediment–water interface. *Environ. Sci. Technol.* **2001**, *35* (1), 192–195.
- (5) Barton, S. C.; Gallaway, J.; Atanassov, P. Enzymatic biofuel cells for implantable and microscale devices. *Chem. Rev.* **2004**, *104* (10), 4867–4886.
- (6) Logan, B. E.; Hamelers, B.; Rozendal, R.; Schröder, U.; Keller, J.; Freguia, S.; Aelterman, P.; Verstraete, W.; Rabaey, K. Microbial fuel cells: Methodology and technology. *Environ. Sci. Technol.* **2006**, *40* (17), 5181–5191.
- (7) Rozendal, R. A.; Hamelers, H. V. M.; Buisman, C. J. N. Effects of membrane cation transport on pH and microbial fuel cell performance. *Environ. Sci. Technol.* **2006**, *40*, 5206–5211.
- (8) Zhao, F.; Harnisch, F.; Schröder, U.; Scholz, F.; Bogdanoff, P.; Herrmann, I. Constraints and challenges of using oxygen cathodes in microbial fuel cells. *Environ. Sci. Technol.* **2006**, *40* (17), 5191–5199.
- (9) Heller, A. Miniature biofuel cells. *Phys. Chem. Chem. Phys.* **2004**, *6*, 209–216.
- (10) Stenina, I. A.; Sista, P.; Rebrov, A. I.; Pourcelly, G.; Yaroslavtsev, A. B. Ion mobility in Nafion-117 membranes. *Desalination* **2004**, *170*, 49–57.
- (11) Schröder, U. Anodic electron transfer mechanisms in microbial fuel cells and their energy efficiency. *Phys. Chem. Chem. Phys.* **2007**, *9*, 2619–2629.
- (12) Rozendal, R. A.; Hamelers, H. V. M.; Molenkamp, R. J.; Buisman, C. J. N. Performance of single chamber biocatalyzed electrolysis with different types of ion exchange membranes. *Water Res.* **2007**, *41*, 1984–1994.
- (13) Liu, H.; Logan, B. E. Electricity generation using an air-cathode single chamber microbial fuel cell (MFC) in the absence of a proton exchange membrane. *ACS, Division of Environmental Chemistry—Preprints of Extended Abstracts* **2004**, *44* (2), 1485–1488.
- (14) Biffinger, J. C.; Ray, R.; Little, B.; Ringeisen, B. R. Diversifying biological fuel cell designs by use of nanoporous filters. *Environ. Sci. Technol.* **2007**, *41* (4), 1444–1449.
- (15) Kim, J. R. C., S.; Oh, S.-E.; Logan, B. E. Power generation using different cation, anion, and ultrafiltration membranes in microbial fuel cells. *Environ. Sci. Technol.* **2007**, *41*, 1004–1009.
- (16) Heijne, A. T.; Hamelers, H. V. M.; de Wilde, V.; Rozendal, R. A.; Buisman, C. J. N. A bipolar membrane combined with ferric iron reduction as an efficient cathode system in microbial fuel cells. *Environ. Sci. Technol.* **2006**, *40*, 5200–5205.
- (17) Koros, W. J.; Ma, Y. H.; Shimidzu, T. Terminology for membranes and membrane processes. *Pure Appl. Chem.* **1996**, *68* (7), 1479–1489.
- (18) Broka, K.; Ekdunge, P. Oxygen and hydrogen permeation properties and water uptake of Nafion 117 membrane and recast film for PEM fuel cell. *J. Appl. Electrochem.* **1997**, *27*, 117–123.
- (19) Song, S. Q.; Zhou, W. J.; Li, W. Z.; Sun, G.; Xin, Q.; Kontou, S.; Tsiakaras, P. Direct methanol fuel cells: Methanol crossover and its influence on single DMFC performance. *Ionics* **2004**, *10* (5–6), 458–462.
- (20) GmbH, F.-T. *Technical Information Sheet Fumasep FBM*; Fumatech, GMBH: Sankt Ingbert, Germany, 2006; p 2.

- (21) Hurwitz, H. D.; Dibiani, R. Investigation of electrical properties of bipolar membranes at steady state and with transient currents. *Electrochim. Acta* **2001**, *47*, 759–773.
- (22) Krol, J. J., *Monopolar and Bipolar Ion Exchange Membranes: Mass Transport Limitations*; Print Partners Ipskamp: Netherlands, Enschede, 1997.
- (23) Hurwitz, H.; D, D., R. Investigation of electrical properties of bipolar membranes at steady state and with transient methods. *Electrochim. Acta* **2001**, 759–773.
- (24) Lteif, R.; Dammak, F.; Larchet, C.; Auclair, B. Conductivite electrique membranaire: etude de l'effet de la concentration, de la nature de l'electrolyte et de la structure membranaire. *Eur. Polym. J.* **1999**, *35*, 1187–1195.
- (25) Unnikrishnan, E. K.; Kumar, S. D.; Maiti, B. Permeation of inorganic anions through Nafion ionomer membrane. *J. Membr. Sci.* **1997**, *137* (1–2), 133–137.
- (26) Rosenbaum, M.; Schröder, U.; Scholz, F. In situ Electrooxidation of Photobiological Hydrogen in a Photobiological Fuel Cell Based on *Rhodobacter sphaeroides* *Environ. Sci. Technol.* **2005**, *39*, (16), 6328–6333.
- (27) Bullen, R. A.; Arnot, T. C.; Lakeman, J. B.; Walsh, F. C. Biofuel cells and their development. *Biosens. Bioelectron.* **2006**, *21* (11), 2015–2045.
- (28) Shukla, A. K.; Suresh, P.; Berchmans, S.; Rajendran, A. Biological fuel cells and their application. *Curr. Sci.* **2004**, *87* (4), 455–468.
- (29) Liu, H.; Logan, B. E. Electricity generation using an air-cathode single chamber microbial fuel cell in the presence and absence of a proton exchange membrane. *Environ. Sci. Technol.* **2004**, *38* (14), 4040–4046.
- (30) Oh, S.; Min, B.; Logan, B. E. Cathode performance as a factor in electricity generation in microbial fuel cells. *Environ. Sci. Technol.* **2004**, *38* (18), 4900–4904.

ES702224A